Geostrophic versus MHD Models

Thierry Alboussière

Laboratoire de Géophysique Interne et Tectonophysique, CNRS, Observatoire de Grenoble, Université Joseph Fourier, Maison des Géosciences, BP 53, 38041 Grenoble Cedex 9, France (thierry.alboussiere@obs.ujf-grenoble.fr)

1 Introduction

Low magnetic Reynolds number MHD flows and low Rossby number rotating flows share a number of common features. Both are subjected to a strong linear force: Lorentz or Coriolis. From an energetic point of view, they are very different, as Lorentz forces are dissipative in nature (Joule dissipation adding to viscous dissipation) while Coriolis forces are purely conservative. Both forces however tend to favour a two-dimensional flow, independent of the direction of the applied magnetic field or rotation axis. This can be seen most easily on steady solutions, where three-dimensional structures are absent in the bulk of the flow. Exactly how these MHD or rotating flows become two-dimensional is very interesting. In MHD flows, due to Joule dissipation, this takes the form of a pseudo-diffusion (Moffatt 1967 [1], or Sommeria and Moreau 1982 [2]), whereby three-dimensional features are diffusively stretched in the direction of the magnetic field, with a pseudo-diffusion coefficient proportional to the square of their size in the perpendicular direction. In rotating flows the process is dominated by inertial waves. Three-dimensional structures give rise to dispersive fast (small Rossby number) inertial waves, whereas nearly two-dimensional structures correspond to inertial waves with a wave-number perpendicular to the rotation axis, hence a vanishing pulsation according to their dispersion relationship (see Greenspan [3] for a complete exposition). Those two-dimensional structures are thus not rapidly dispersed and remain alone eventually. Historically, the tendency towards two-dimensional flows in rotating systems has been suggested and demonstrated experimentally by Proudman [4] and Taylor [5, 6].

Having established the two-dimensional nature of these flows, it was then natural to derive two-dimensional flow equations. For rotating flows, Montgomery 1938 [7] pointed out the role of the so-called geostrophic contours (constant depth in the direction of rotation in the case of uniform density): this follows from the conservation of the background angular momentum. If the flow departs slightly from those contours, this is a source of vorticity in the

rotating frame of reference. The contribution of Ekman layers was recognized following Ekman [8]: for the case of a solid boundary, they are also a source (or rather a sink) of vorticity associated to Ekman pumping. Finally, the core two-dimensional viscosity is also "dissipating" enstrophy. When the material derivative of the vorticity is expressed in terms of these above-mentioned three contributions, the equation of the so-called homogeneous model for rotating flows is obtained. This has been used for modelling oceanic circulation (Greenspan [3]): some typical boundary layers arising from this model have been invoked to represent western streams such as the Gulf stream or the Kuroshio stream. Stewartson [9, 10] played an important role in analyzing shear layers developing on singular surfaces parallel to the rotation axis.

In parallel, progress has been made in the understanding of the behaviour of electrically conducting fluids in the presence of an imposed magnetic field. Hartmann and Lazarus 1937 [11] discovered Hartmann layers, the boundary layer analogue to the Ekman layer and responsible for an increase in wall friction. Another type of layers, parallel to the direction of the magnetic field and an analogue to Stewartson layers, has been put in evidence by Shercliff 1953 [12] first. Kulikovskii 1958 [13] made a major contribution when he launched the concept of "characteristic surfaces", analogous to the geostrophic contours. Characteristic surfaces are made of magnetic lines with a constant ratio of magnetic field intensity divided by the line length. Magnetic circulation is conserved for flows following these surfaces. Otherwise, in case of cross flow, vorticity is generated by the electrical currents created by the variations in magnetic circulation. Holroyd and Walker 1978 [14] have written inertialess two-dimensional equations, which were only recently put under a form similar to the rotating homogeneous model and analyzed in terms of potential two-dimensional structures [15].

The similarity between rotating and MHD flows will be emphasized here as much as it is possible, so as to benefit from all advances in either field. More efforts have gone into rotating flows, and they are perhaps slightly easier to handle as there is only one equation to consider (Navier-Stokes) while Ohm's law has to be combined with Navier-Stokes in MHD studies. There has seemed that rotating flows could show a greater variety of shear layers. Using the analogy between both types of flows, one can either find the corresponding MHD layers or find a good reason why the corresponding layer is not physical.

In §2, the fundamental length-scales arising in rotating or MHD flows will be introduced. §3 will be devoted to the derivation of the homogeneous model of rotating flows. An MHD two-dimensional model is derived in §4. The next §5 will provide an example of a two-dimensional MHD flow calculated from the model just derived. Finally conclusions and perspectives will be presented in §6.

2 Fundamental length-scales

Starting from the governing equations of rotating and MHD flows respectively, fundamental scales will be identified and used to justify the subsequent two-dimensional models to be introduced in the second stage.

2.1 Rotating flows

Fluid motion in a reference system rotating with a steady angular velocity $\mathbf{\Omega}$ is subjected to apparent forces, Coriolis and centrifuge. While centrifuge forces can be absorbed in a modified pressure term, Coriolis forces have to be considered specifically as they play a distinct role. Momentum, or Navier-Stokes equation, with Coriolis forces, is the governing equation for the solenoidal velocity field $\mathbf{u}$. This equation takes the following dimensionless form:

$$\frac{\partial \mathbf{u}}{\partial t} + (\mathbf{u}\cdot\boldsymbol{\nabla})\mathbf{u} = -\boldsymbol{\nabla} p + 2\,E^{-1}\,\mathbf{u}\times\mathbf{e}_z + \boldsymbol{\nabla}^2\mathbf{u}, \tag{1}$$

where dimensionless vector position $\mathbf{x}$, time t, velocity field $\mathbf{u}$ and pressure field p are derived from their corresponding dimensional quantities using the scales H, H^2/ν, ν/H and $\rho\nu^2/H^2$, respectively. Here H is a length-scale of the fluid domain, ρ the density of the fluid and ν its kinematic viscosity. The Ekman number appearing in the equation is defined as $E = \nu/(\Omega H^2)$. Reference axes have been chosen so that the rotation axis lies in the z-direction and $\mathbf{e}_z$ denotes the unit vector along the z direction.

It is possible to extract fundamental time and length-scales from the governing equation. Taking the curl of Eq. (1) eliminates the pressure:

$$\frac{\partial \boldsymbol{\nabla}\times\mathbf{u}}{\partial t} + \boldsymbol{\nabla}\times[(\mathbf{u}\cdot\boldsymbol{\nabla})\mathbf{u}] = 2\,E^{-1}\,\frac{\partial \mathbf{u}}{\partial z} + \boldsymbol{\nabla}^2\,(\boldsymbol{\nabla}\times\mathbf{u})\,. \tag{2}$$

In the asymptotic limit of strong rotation ($E \longrightarrow 0$), the first term on the right-hand side of Eq. (2) is dominant and can be balanced by the first term (time derivative) of the left-hand side when a short time-scale E is invoked, i.e. the time for the reference system to rotate an angle of one radian. These two terms are responsible for the inertial waves, which satisfy the following dispersion relationship:

$$\omega = \pm 2E^{-1}\cos\theta, \tag{3}$$

where the velocity of inertial modes is defined as $\mathbf{u} = \mathbf{u}_0\; e^{i(\omega t + \mathbf{k}\cdot\mathbf{x})}$ and where θ is the angle between $\mathbf{k}$ and $\mathbf{\Omega}$. After a transient period of inertial wave propagation, the final state of the flow corresponds to a quasi-steady two-dimensional state ($\theta \simeq \pi/2$, hence $\omega \simeq 0$). These inertial waves can be disrupted by non-linear inertial terms (the second term on the left-hand side), provided the Rossby number is not small compared to unity. In our dimensionless formulation, the Rossby number is the product of the dimensionless velocity with the Ekman number, while it is $Ro = U/(\Omega H)$ when U denotes

a dimensional velocity scale. Viscous effects (second term on the right-hand side) can also affect inertial waves by viscous damping and are responsible for thin shear layers in the steady or quasi-steady state: $E^{1/2}$ Ekman layers along boundaries not parallel to the rotation direction and $E^{1/3}$ Stewartson layers developing along surfaces containing the rotation direction. Finally, the condition for the existence of a quasi-steady two-dimensional flow is that of a small Rossby number only for regions outside Ekman and $E^{1/3}$ Stewartson layers. These conditions will be used a posteriori to assess the validity of two-dimensional solutions.

2.2 MHD flows

In MHD flows, our attention will be restricted here to the case of low magnetic Reynolds numbers. Momentum equation and Ohm's law are the two governing equations, expressed in a dimensionless form:

$$\frac{\partial \mathbf{u}}{\partial t} + (\mathbf{u}\cdot\boldsymbol{\nabla})\mathbf{u} = -\boldsymbol{\nabla} p + Ha^2\,\mathbf{j}\times\mathbf{B} + \boldsymbol{\nabla}^2\mathbf{u}, \tag{4}$$

$$\mathbf{j} = -\boldsymbol{\nabla}\phi + \mathbf{u}\times\mathbf{B}. \tag{5}$$

Dimensional scales already defined above for rotating flows are still valid. In addition, the dimensionless electric current density $\mathbf{j}$ and electric potential field ϕ are obtained from their dimensional counterpart using the scales $\nu\sigma B_0/H$ and νB_0, where B_0 is a typical value of the imposed magnetic field.

To obtain an equation for the velocity field $\mathbf{u}$ suitable for analysis, one can take the curl of the momentum equation twice and substitute $\boldsymbol{\nabla}\times\mathbf{j}$ using the curl of Ohm's law:

$$\frac{\partial}{\partial t}\left(-\boldsymbol{\nabla}^2\mathbf{u}\right) + \boldsymbol{\nabla}\times\boldsymbol{\nabla}\times[(\mathbf{u}\cdot\boldsymbol{\nabla})\mathbf{u}] = Ha^2\,\frac{\partial^2\mathbf{u}}{\partial z^2} - \left(\boldsymbol{\nabla}^2\right)^2\mathbf{u}. \tag{6}$$

This equation is obtained using the approximation of a locally uniform magnetic field. This is not exact but this does not affect the following scaling analysis. The asymptotic strong MHD regime is characterized by a large value of the Hartmann number ($Ha \longrightarrow \infty$). The dominant first term on the right-hand side of Eq. (6) can only be balanced by the first term (time derivative) on the left-hand side on a short timescale of order Ha^{-2}, i.e. the so-called Joule time $\rho/(\sigma B^2)$. These two terms define an equation of pseudo-diffusion for the velocity field. Its dispersion relationship takes the following form:

$$\omega = iHa^2\frac{(\mathbf{k}.\mathbf{B})^2}{k^2}, \tag{7}$$

for elementary solutions defined as $\mathbf{u} = \mathbf{u}_0\, e^{i(\omega t + \mathbf{k}\cdot\mathbf{x})}$. This is similar to the dispersion relationship of an equation of diffusion, but with a diffusion coefficient D dependent on the length-scale l of the velocity disturbance $D \simeq Ha^2 l^2$. The ultimate state of pseudo-diffusion is a quasi-steady two-dimensional flow. The

non-linear inertial term (the second one on the right-hand side of Eq. (6)) can disrupt this pseudo-diffusion process provided the interaction parameter N is small compared to unity. In our dimensionless formulation, the interaction parameter is defined as the square of the ratio of the Hartmann number by the dimensionless velocity, or $N = \sigma B_0^2 H/(\rho U)$ using the dimensional scale U for the velocity. Viscous terms (the last term in Eq. (6)) provide additional diffusion to the MHD pseudo-diffusion and are responsible for the existence of thin shear layers in the steady state: Ha^{-1}-thick Hartmann layers on walls non parallel to the magnetic field and $Ha^{-1/2}$-thick so-called "parallel" layers developing along surfaces made of magnetic lines. Two dimensional models will be valid for a large value of the interaction parameter and will apply outside Hartmann or parallel layers.

3 The "homogeneous model" of rotating flows

This model has been developed initially to model oceanic circulation for which the thin aspect ratio (depth over horizontal scales) gives another reason, in addition to rotation effects, to focus on two-dimensional flows. This aspect ratio condition is not necessary and the homogeneous model has also been applied to other geometries, e.g. to the thick atmosphere of Jupiter or to the Earth's liquid inner core.

Let us assume for simplicity that the fluid domain is symmetrical with respect to a plane perpendicular to the axis of rotation. A two-dimensional model arises naturally for the long time evolution of flows in rotating systems if one considers Eq. (2) and the fact that the fluid domain is bounded in the direction of the rotation axis. From this last condition, it is concluded that the strongest flow components will be perpendicular to the rotation axis. This follows from continuity as Ekman layers cannot accept a jump in the normal component but only a jump in the tangential components of velocity. Hence, the two-dimensional flow is a flow with two-dimensional flow components in the direction perpendicular to the axis of rotation. From Eq. (2), the flow component parallel to the rotation axis is odd with respect to the plane of symmetry and small compared to perpendicular components. The main component of vorticity is parallel to the axis of rotation and is two-dimensional.

Traditionally, the homogeneous model is derived from the equation of vorticity, projected on the direction of the rotation axis. Sources of vortex stretching are due to two causes: geometrical effects and Ekman pumping. If the depth of the fluid domain changes in the direction of the two-dimensional flow, axial stretching or compression must occur so that the core flow remains tangent to the upper and lower boundaries. Regarding Ekman layers developing at a solid boundary, there is a fundamental linear relationship between the normal flow velocity entering the layer and the vorticity of the two-dimensional flow.

We are going to present a slightly different derivation based on global conservation, Ekman layer properties and analysis of the two-dimensional core flow. The geometry of the cavity consists of the space situated between two symmetrical surfaces, defined in the orthonormal coordinate system (x, y, z) by the two functions, $z^u(x, y)$ and $-z^u(x, y)$, respectively, where z is still referring to the direction of the axis of rotation. The "depth" of the cavity is defined as the distance between both surfaces as a function of x and y, $d(x, y) = 2z_u(x, y)$. Assuming the existence of a core flow were x and y components of the flow are independent of z, a purely two-dimensional flow $\mathbf{u}_0$ with no z component is introduced:

$$\mathbf{u}_0 = \begin{bmatrix} u_{0x}(x, y) \\ u_{0y}(x, y) \end{bmatrix}. \tag{8}$$

One must be careful as this is not the real flow and, for instance, this flow need not be divergence-free. However, in the absence of flow injection through the upper and lower boundaries, global volume conservation implies that the two-dimensional mass flow rate, denoted $\mathbf{Q}(x, y)$, is a divergence-free two-dimensional vector field. It is attributed a streamfunction, ψ:

$$\mathbf{Q} = \boldsymbol{\nabla}\psi \times \mathbf{e}_z. \tag{9}$$

One has to link $\mathbf{Q}$ to $\mathbf{u}_0$, taking into account the effect of the upper and lower Ekman layers. These layers contribute a small flow deficit in the direction of the core flow, but more importantly, they generate a component of cross-flow due to Ekman pumping. This cross-flow is small but has important consequences in terms of mass conservation: a vortex core flow creates a purely divergent cross-flow in Ekman layers. In our dimensionless formulation, the cross-flow is equal to $E^{1/2}\mathbf{e}_z \times \mathbf{u}_0$, so that the global two-dimensional flow can be written:

$$\mathbf{Q} = d\,\mathbf{u}_0 + E^{1/2}\mathbf{e}_z \times \mathbf{u}_0. \tag{10}$$

Finally, one must write the restriction of the momentum Eq. (1) to the x and y components in the core of the flow, in terms of the two-dimensional vector field $\mathbf{u}_0$ and the pressure field $p = p_0(x, y)$ at $z = 0$:

$$\frac{\partial \mathbf{u}_0}{\partial t} + (\mathbf{u}_0 \cdot \boldsymbol{\nabla})\mathbf{u}_0 = -\boldsymbol{\nabla} p_0 + 2\,E^{-1}\mathbf{u}_0 \times \mathbf{e}_z + \boldsymbol{\nabla}^2\mathbf{u}_0. \tag{11}$$

Let us denote the single component (in the direction of the rotation axis) of the curl of $\mathbf{u}_0$ by ω_0. We shall take the curl of the restricted momentum Eq. (11), bearing in mind that all variables are two-dimensional:

$$\frac{\partial \omega_0}{\partial t} + \mathbf{u}_0 \cdot \boldsymbol{\nabla}\omega_0 + (\boldsymbol{\nabla} \cdot \mathbf{u}_0)\omega_0 = -2\,E^{-1}(\boldsymbol{\nabla} \cdot \mathbf{u}_0) + \nabla^2\omega_0. \tag{12}$$

The divergence of $\mathbf{u}_0$ can be expressed from the two-dimensional divergence of Eq. (10), where $\mathbf{Q}$ is solenoidal:

$$\boldsymbol{\nabla}\cdot\mathbf{Q} = d\,\boldsymbol{\nabla}\cdot\mathbf{u}_0 + \mathbf{u}_0\cdot\boldsymbol{\nabla}d - E^{1/2}\omega_0 = 0, \tag{13}$$

hence

$$\boldsymbol{\nabla}\cdot\mathbf{u}_0 = -\frac{1}{d}\mathbf{u}_0\cdot\boldsymbol{\nabla}d + E^{1/2}\frac{\omega_0}{d}. \tag{14}$$

In the first term of the right-hand side, one can express $\mathbf{u}_0$ with $\mathbf{Q}$ at the leading order: $\mathbf{u}_0 = \mathbf{Q}/d$. Eq. (14) becomes:

$$\boldsymbol{\nabla}\cdot\mathbf{u}_0 = \mathbf{Q}\cdot\boldsymbol{\nabla}\left(\frac{1}{d}\right) + E^{1/2}\frac{\omega_0}{d}, \tag{15}$$

where the small $E^{1/2}\omega_0/d$ term is necessarily retained as $\boldsymbol{\nabla}\cdot\mathbf{u}_0$ will be multiplied by the large E^{-1} factor in Eq. (12). Next, the non-linear term $\mathbf{u}_0\cdot\boldsymbol{\nabla}\omega_0$ will be approximated using $\mathbf{u}_0 \simeq \mathbf{Q}/d$ so as to retain only consistent orders of magnitude in a $E^{1/2}$ Taylor expansion. Eq. (12) can finally be written as follows:

$$\frac{\partial\omega_0}{\partial t} + \boldsymbol{\nabla}\left(\frac{\omega_0}{d}\right)\times\boldsymbol{\nabla}\psi = -2\,E^{-1}\boldsymbol{\nabla}\left(\frac{1}{d}\right)\times\boldsymbol{\nabla}\psi - 2E^{-1/2}\frac{\omega_0}{d} + \nabla^2\omega_0. \tag{16}$$

Note that all terms are scalars in the two-dimensional equation above: cross-products are identified with their single non-zero z-component. Note also that vorticity transport and geometrical vortex stretching have been combined into a single term: $\boldsymbol{\nabla}\omega_0\times(\boldsymbol{\nabla}\psi/d) + \omega_0\boldsymbol{\nabla}(1/d)\times\boldsymbol{\nabla}\psi = \boldsymbol{\nabla}(\omega_0/d)\times\boldsymbol{\nabla}\psi$. These are local vorticity terms, not planetary or background vorticity. Finally, as we have carefully retained dominant terms in the vorticity equation above, we can again use $\mathbf{u}_0 \simeq \mathbf{Q}/d$ to express vorticity in terms of the streamfunction ψ:

$$\omega_0 = -\boldsymbol{\nabla}\cdot\left(\frac{\boldsymbol{\nabla}\psi}{d}\right). \tag{17}$$

The two-dimensional Eqs. (16) and (17) constitute the so-called homogeneous model of quasi-geostrophic flows.

The homogeneous model can be entered into a numerical formulation, and quasi-geostrophic flows can be computed. Here we shall only have a look at this model to identify some expected features. In a steady or quasi-steady low-Rossby number regime, there can be a competition between the last two terms (dissipation by Ekman layer friction or bulk two-dimensional viscous dissipation), which results in the development of $E^{1/4}$ thick Stewartson layers. This feature is legitimate in the quasi-geostrophic model, as $E^{1/4}$ is thicker than $E^{1/3}$: as it is recalled in §2.1, the length-scales perpendicular to the rotation axis of the order $E^{1/3}$ or smaller are not associated with two-dimensional structures, but to three-dimensional ones. Apart from Stewartson layers, there can be Munk layers [16] when topography effects exist: the first and last terms at the right-hand side of Eq. (16) compete on a length-scale $E^{1/3}\beta^{-1/3}$, where β is the magnitude of $\boldsymbol{\nabla}(1/d)$. When β is very small compared to unity, this length-scale is large compared to $E^{1/3}$ and corresponds to a valid

quasi-geostrophic flow structure. When unsteady solutions are considered, the easiest case is that of a balance between the time-dependent term and the dominant term in Ekman number expansion, that of planetary vortex stretching. Considering local coordinates (x,y) such that the depth d is constant along the x direction, this balance in Eq. (16) can be written as follows:

$$\frac{\partial \omega_0}{\partial t} = 2\,E^{-1}\beta\frac{\partial \psi}{\partial x}. \tag{18}$$

This equation is generating the so-called Rossby waves. When β is small compared to unity, homogeneous elementary solutions $e^{i\omega t+i\mathbf{k}\cdot\mathbf{x}}$ must satisfy:

$$\omega = 2\,E^{-1}\beta\frac{k_x}{k^2}. \tag{19}$$

These waves live in two dimensions and are slower than inertial waves. Rossby waves are indeed the trace of inertial waves in the two-dimensional plane perpendicular to the axis of rotation.

4 A two-dimensional MHD model

The derivation of a two-dimensional MHD model presented here follows very closely the presentation of the model of homogeneous rotating flows above. Global two-dimensional conservation laws (for mass and electric charge) are combined to the evolution equation for vorticity and electric current in the bulk of the fluid to provide two coupled governing equations.

The magnetic field is supposed to lie in the z-direction, but its intensity can now be a function of x and y, $B_z = B_z(x,y)$: this is known as the "straight magnetic lines approximation". As a first step, we consider that the "horizontal" components (perpendicular to $\mathbf{B}$) of the velocity and also of the electric current density are independent of z in the bulk of the fluid:

$$\mathbf{u}_0 = \begin{bmatrix} u_{0x}(x,y) \\ u_{0y}(x,y) \end{bmatrix}, \qquad \mathbf{j}_0 = \begin{bmatrix} j_{0x}(x,y) \\ j_{0y}(x,y) \end{bmatrix}. \tag{20}$$

The two-dimensional integrated volume flow rate is still denoted $\mathbf{Q}(x,y)$ and we introduce also the two-dimensional integrated electric current density $\mathbf{I}(x,y)$. We shall then consider the two-dimensional mass and electric charge conservation laws after integration along z over the total depth $d(x,y)$ of the cavity (from the lower wall $z=-z_u(x,y)$ to the upper wall $z=z_u(x,y)$). This implies the existence of two streamfunctions:

$$\mathbf{Q} = \boldsymbol{\nabla}\psi \times \mathbf{e}_z, \qquad \mathbf{I} = \boldsymbol{\nabla}h \times \mathbf{e}_z, \tag{21}$$

where the variable name $h(x,y)$ for the electric current streamfunction recalls us that this is indeed the induced magnetic field in the z direction. The next

step is to express the two-dimensional, integrated fluxes in terms of a bulk flow contribution (20) and a contribution from Hartmann layers. In MHD, the flow deficit in Hartmann layers is of little importance. The electric current developing in them is the important feature (Shercliff [12]):

$$\mathbf{Q} = d\,\mathbf{u}_0, \qquad \mathbf{I} = d\,\mathbf{j}_0 + 2\,Ha^{-1}B_z\mathbf{e}_z \times \mathbf{u}_0, \tag{22}$$

written here for the case of a slowly varying depth $\partial d/\partial x << 1, \partial d/\partial y << 1$. We then consider the restriction of the momentum Eq. (4) and of Ohm's law (5) to the x and y components in the core of the flow, in terms of the two-dimensional vector fields $\mathbf{u}_0$, $\mathbf{j}_0$ and pressure and electric potential fields at $z = 0$, $p = p_0(x, y)$, $\phi = \phi_0(x, y)$:

$$\frac{\partial \mathbf{u}_0}{\partial t} + (\mathbf{u}_0 \cdot \boldsymbol{\nabla})\mathbf{u}_0 = -\boldsymbol{\nabla} p_0 + Ha^2 B_z \mathbf{j}_0 \times \mathbf{e}_z + \boldsymbol{\nabla}^2 \mathbf{u}_0, \tag{23}$$

$$\mathbf{j}_0 = -\boldsymbol{\nabla}\phi + B_z \mathbf{u}_0 \times \mathbf{e}_z. \tag{24}$$

Taking the curl of these two-dimensional equations leads to:

$$\frac{\partial \omega_0}{\partial t} + \mathbf{u}_0 \cdot \boldsymbol{\nabla}\omega_0 + (\boldsymbol{\nabla} \cdot \mathbf{u}_0)\omega_0 = -Ha^2 \boldsymbol{\nabla} \cdot (B_z \mathbf{j}_0) + \nabla^2 \omega_0, \tag{25}$$

$$\boldsymbol{\nabla} \times \mathbf{j}_0 = -\boldsymbol{\nabla} \cdot (B_z \mathbf{u}_0). \tag{26}$$

From the expressions (22), divergence terms in the equations above can be written:

$$\boldsymbol{\nabla} \cdot (B_z \mathbf{j}_0) = (\mathbf{I} \cdot \boldsymbol{\nabla}) \left(\frac{B_z}{d} \right) + 2Ha^{-1} \mathbf{e}_z \cdot \boldsymbol{\nabla} \times \left(\frac{B_z}{d^2} \mathbf{Q} \right), \tag{27}$$

$$\boldsymbol{\nabla} \cdot (B_z \mathbf{u}_0) = (\mathbf{Q} \cdot \boldsymbol{\nabla}) \left(\frac{B_z}{d} \right), \tag{28}$$

which can be substituted into the two-dimensional governing Eqs. (23) and (24). Using the streamfunctions ψ and h defined by Eq. (21), the governing equations are finally written:

$$\frac{\partial \omega_0}{\partial t} + \boldsymbol{\nabla} \left[\frac{\omega_0}{d} \right] \times \boldsymbol{\nabla}\psi = Ha^2 \boldsymbol{\nabla} \left[\frac{B_z}{d} \right] \times \boldsymbol{\nabla} h + 2Ha \boldsymbol{\nabla} \cdot \left[\frac{B_z}{d^2} \boldsymbol{\nabla}\psi \right] + \nabla^2 \omega_0, \tag{29}$$

$$-\boldsymbol{\nabla} \cdot \left[\frac{1}{d} \boldsymbol{\nabla} h \right] = \boldsymbol{\nabla} \left[\frac{B_z}{d} \right] \times \boldsymbol{\nabla}\psi, \tag{30}$$

where Eq. (17) relating ω_0 and ψ is still valid here, in the MHD context.

These governing Eqs. (29), (30) and (17) will be discretized and solved numerically in the next §5 for a particular configuration. Let us here first analyze these equations from a general point of view in the same way as for the homogeneous model of rotating flows. One can first look at the structures arising from the balance of bulk viscosity and Hartmann layer friction,

i.e. between the last two terms in Eq. (29). By scaling analysis, this corresponds to shear layers of thickness $Ha^{-1/2}$. This corresponds to the typical thickness of parallel layers (see §2). This does not mean however that we are representing parallel layers well with the two-dimensional model. On the contrary, we know that structures developing on a length-scale of unity in the direction of the magnetic field and on a length-scale $Ha^{-1/2}$ or less in a direction perpendicular to the magnetic field are essentially three-dimensional. We may obtain a solution looking like a parallel layer, but this is just an approximation. And this approximation does not become any more accurate as the Hartmann number is increased. As a corollary, we may just remove the last term (bulk viscosity) from Eq. (29) as it will always be negligible compared to the term before (Hartmann layer friction), as long as legitimate two-dimensional structures are modelled. The situation has to be contrasted with that of rotating flows for which a similar balance had provided a legitimate $E^{1/4}$ length-scale (two-dimensional Stewartson layers), larger than three-dimensional $E^{1/3}$ Stewartson layers[1].

For steady, high interaction parameter flows, one may examine the balance between Hartmann layer friction and the first term on the right-hand side of Eq. (29), representing a source of vorticity as the electric current passes across characteristic surfaces (B_z/d constant). To do so, we must use the electric Eq. (30), expressing the fact that curl is generated for the two-dimensional current when the two-dimensional flow passes across characteristic surfaces. In order to combine more easily Eqs. (29) and (30), it will be useful to write them in local coordinates (x, y), such that the characteristic function B_z/d is constant along the x axis. In the steady, inertialess regime, denoting the magnitude of $\boldsymbol{\nabla}(B_z/d)$ by G and neglecting other variations of B_z and d for simplicity, the governing two-dimensional equations take the following form:

$$0 = -Ha^2 G\frac{\partial h}{\partial x} + 2Ha\frac{B_z}{d^2}\nabla^2\psi, \tag{31}$$

$$-\frac{1}{d}\,\nabla^2 h = -G\frac{\partial \psi}{\partial x}. \tag{32}$$

Taking the Laplacian of Eq. (31) and substituting h using Eq. (32), one gets a local equation for ψ, bearing in mind that all variations of B_z and d have been discarded, except obviously when building G:

$$-HaG^2 d\frac{\partial^2 \psi}{\partial x^2} + 2\frac{B_z}{d^2}\nabla^4\psi = 0. \tag{33}$$

This balance shows that shear layers of thickness $Ha^{-1/4}G^{-1/2}$ and length unity can develop along characteristic surfaces, as illustrated in [15]. This equation can also be used to derive the development length $Ha^{1/2}G$ observed

[1] The fact that both structures have been discovered by Stewartson and named after him does not help to distinguish them.

for instance in pressure-driven flows in cylinders with a step transverse magnetic field. Another outcome of Eq. (33) takes the form of boundary layers along walls cutting characteristic surfaces. They are equivalent to Munk layers in rotating fluids, or rather Stommel layers [17], as the balance in Eq. (33) involves topographic effects and Hartmann layer friction. In this case, scaling analysis of Eq. (33) provides a typical thickness $Ha^{-1/2}G^{-1}$. When $G << 1$, this scaling is legitimate with respect to the two-dimensional nature of the solution. In reality, there is probably a double layer structure in most practical cases, with a genuine $Ha^{-1/2}$ (three-dimensional) parallel sublayer within this thicker $Ha^{-1/2}G^{-1}$ two-dimensional layer. The steady features above have been described in more details in [18, 15].

Finally, one can take a look at the unsteady two-dimensional regime in the simplest regime of negligible non-linear inertial terms. The time-dependent term in Eq. (29) is balanced by the dominant term in terms of Hartmann number expansion, $Ha^2 \boldsymbol{\nabla} [B_z/d] \times \boldsymbol{\nabla} h$. Using again the local coordinates defined above, and neglecting variations of B_z and d, the following equation can be derived:

$$\frac{1}{d}\frac{\partial}{\partial t} \left(\nabla^2\right)^2 \psi = Ha^2 G^2 d \frac{\partial^2 \psi}{\partial x^2}.$$

Solutions to this equation are the counterpart of Rossby waves in rotating fluids. Starting from elementary $e^{i\omega t + i\mathbf{k}\cdot\mathbf{x}}$ the dispersion equation is:

$$\omega = i Ha^2 G^2 d^2 \frac{k_x^2}{k^4}, \tag{34}$$

typical of a pseudo-diffusion equation. This is obviously reminiscent of the three-dimensional pseudo-diffusion in the direction of the magnetic field. For two-dimensional flows, this has become pseudo-diffusion in the direction of the characteristic surfaces, with a pseudo-diffusion coefficient, $Ha^2 G^2 d^2 l^4$, where l is the typical size of the structure considered. When G is very small compared to unity, this pseudo-diffusion coefficient is small compared to that of three-dimensional MHD pseudo-diffusion.

5 A flow in a spatially-varying magnetic field

This section will be devoted to an example of an MHD two-dimensional flow, calculated numerically from Eqs. (29), (30) and (17). As can be seen in Fig. 1, the configuration is that of a duct of a rectangular cross-section with a (smooth) step transverse magnetic field. Two apparently slightly different configurations will be considered: one in which the shape of the duct is strictly rectangular and another one in which, downstream the magnetic field change, the top and bottom duct walls are slightly curved. The difference lies in the fact that characteristic surfaces are degenerate in the first case, while characteristic surfaces are well defined and aligned with the mean flow direction in the second case, downstream the magnetic field step.

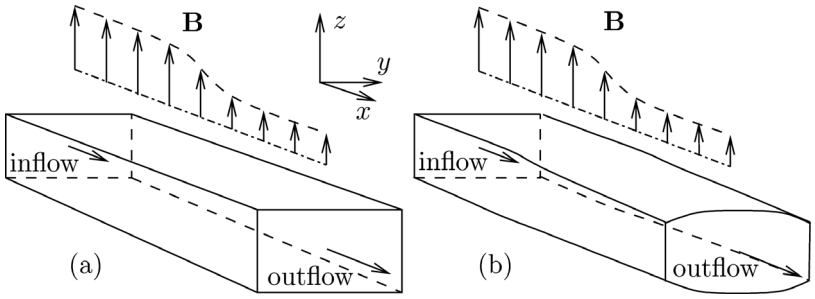

Fig. 1. Rectangular ducts with transverse step magnetic field: (a) flat case, (b) curved case

To be more specific, the width of the duct is equal to 2 in dimensionless terms while its length is 24, from $x = -6$ to $x = 18$, the change in magnetic field intensity taking place between $x = -2$ and $x = +2$:

$$\begin{aligned} B_z &= 0.2, & for \quad & x \geq 2, \\ B_z &= 1 - 0.6x + 0.05x^3, & for \quad & -2 \leq x \leq 2, \\ B_z &= 1.8, & for \quad & x \leq -2, \end{aligned} \tag{35}$$

ensuring a smooth magnetic field and first derivative for all values of x. The depth of the duct in the direction of the magnetic field is uniform and equal to 1 for the first case (a), and varies in the following way for case (b):

$$\begin{aligned} d &= 1, & for \quad & x \leq -2, \\ d &= 1 - (0.25 + 0.1875x - 0.015625x^3)y^2, & for \quad & -2 \leq x \leq 2, \\ d &= 1 - 0.5y^2, & for \quad & x \geq 2. \end{aligned} \tag{36}$$

Fig. 2 shows lines of constant value for the characteristic function B_z/d for both configurations (a) and (b), in the (x, y) plane. Numerical simulations have been run for a single value of the Hartmann number, $Ha = 5 \times 10^3$, and increasing values of the Reynolds number (see Fig. 2). In these simulation, the small bulk viscous term has been retained but boundary conditions at $y = \pm 1$ are free-slip conditions for the velocity field. A no-slip condition would be numerically more demanding as the parallel layers would cause considerable mesh refinement. Moreover we are not particularly interested in $Ha^{-1/2}$ parallel layers in this study. The smallest value of Reynolds number corresponds to an inertialess solution. In the region of varying magnetic field, the flow goes through boundary layers, as expected [15], scaling like $Ha^{-1/2}G^{-1}$ as discussed in the previous section. For larger values of the Reynolds number, a clear asymmetry appears between upstream and downstream regions on each side of the magnetic field change. Upstream the flow is quite similar to the inertialess case, while downstream the wall jets, generated in the non-uniform

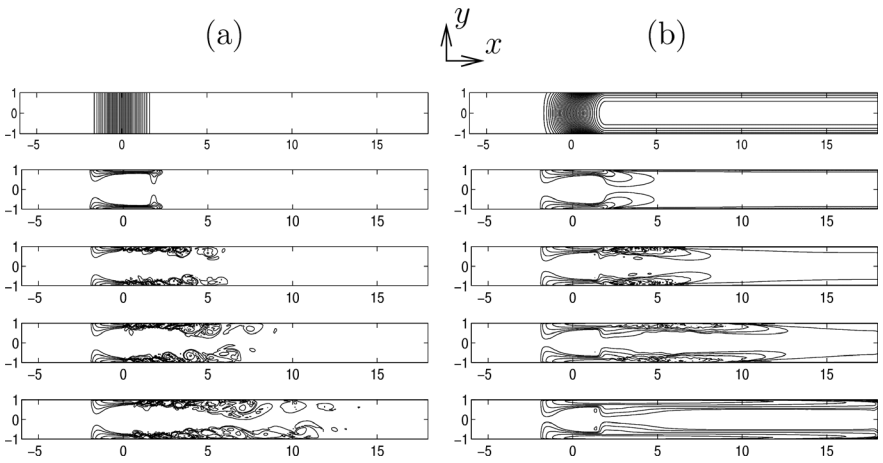

Fig. 2. Isovalues of the characteristic function B_z/d (top), vorticity isolines for increasing Reynolds, $Re = 5$, 10^3, 2×10^3 and 4×10^3: (a) flat case, (b) curved case

region of magnetic field, remain and undergo instability. These instabilities lead to vortices, eventually damped by Hartmann layer friction.

The difference between cases (a) and (b) is visible in the behaviour of the wall jets. In Fig. 2, snapshots of the vorticity isovalues are shown in the final statistically steady regime. For the case (a) of a strictly rectangular duct, the jets undergo shear instability and mixing is rather efficient. For the case (b) of non-uniform duct depth, the characteristic surfaces channel the jets and delay their instability, so that these jets survive further downstream. As discussed in the previous section, vortices are stretched along the x direction by pseudo-diffusion, which is probably at the origin of the observed stabilization of the jets. Their flow direction coincides with the orientation of the surface layers which helps them to propagate further downstream.

6 Conclusions and perspectives

Rotating and MHD flows have been compared for a long time. The comparison is extended here to show that the two-dimensional models can be derived within the same framework in both cases. The two-dimensional equations are different indeed but they both indicate that the evolution of (local) vorticity is subjected to four effects: (1) non-linear transport and stretching of local vorticity, (2) "topographic" constraint, related to the conservation of background circulation or magnetic circulation, (3) Ekman or Hartmann layer friction, and (4) two-dimensional bulk viscosity. These terms involve different derivation orders and their magnitude have different scalings with respect to the Ekman or Hartmann number. Hence, various shear layers can arise with a

range of different thicknesses. Attention must be paid to the lower acceptable size for these two-dimensional structures, $Ha^{-1/2}$ for MHD flows, and $E^{1/3}$ for rotating flows, under which structures are necessarily three-dimensional.

We have also discussed the unsteady behaviour of two-dimensional flows. Rossby waves dominate two-dimensional rotating flows unless there is no topographic (or beta-plane) effect. Correspondingly, we have shown here that two-dimensional unsteady MHD flows are subjected to pseudo-diffusion in the direction of characteristic surfaces, unless there is no topography and the magnetic field is uniform[2]. These unsteady two-dimensional features can be linked to the basic unsteady features of the three-dimensional flows. Inertial waves responsible for the two-dimensional nature of rotating flows reappear as Rossby waves in the (imperfectly) two-dimensional beta-plane configuration. Similarly, pseudo-diffusion responsible for the two-dimensional nature of MHD flows has a pseudo-diffusion reminiscence in the two-dimensional MHD equations.

The analysis of the MHD equations has been restricted here to the case of electrically insulating boundaries. It would be interesting to extend this work to electrically conducting boundaries for practical applications, as done by Bühler and Molokov [19]. Another interesting extension for practical applications (e.g. cooling by liquid metal films of fusion reactors) would be to study the effect of a free surface flow, as initiated by Molokov [20]. Combining MHD two-dimensional modelling and free surface analysis should result in a "shallow water" model for MHD flows.

Let us mention other effects not included in the present work which can affect MHD flows. Inertial effects can become significant in the Hartmann layers themselves at sufficiently high Reynolds number. This causes the appearance of Ekman pumping within the Hartmann layers. In consequence, the two-dimensional equations contain an extra term. This effect has been studied by Pothérat et al [21] and by Dellar [22] in the absence of topography. One can even go a step further and consider the effects of instability [23] and transition to turbulence [24] in Hartmann layers. One can envisage the possibility of a two-dimensional flow with turbulent Hartmann layers. This is analogous to the case of atmospheric or oceanic studies where a turbulent Ekman layer is adjacent to a two-dimensional large-scale flow.

From a theoretical point of view, an important question is related to the nature of the MHD two-dimensional turbulence under the effect of the pseudo-diffusive effects described above. As we know, beta-plane turbulence, studied initially by Rhines [25] departs very significantly from pure two-dimensional turbulence. This turbulence is characterized by a mixture of non-linear inertial terms and linear Rossby waves. Not much has been done so far to characterize two-dimensional MHD turbulence, in the presence of topography or non-uniform magnetic fields.

[2] By the way, this shows that the case of a uniform transverse magnetic field and parallel walls constitutes a very singular case.

References

1. Moffatt HK (1967) On the suppression of turbulence by a uniform magnetic field. J Fluid Mech 28(3):571–592
2. Sommeria J, Moreau R (1982) Why, how, and when, MHD turbulence becomes two-dimensional. J Fluid Mech 118:507–518
3. Greenspan HP (1968) The theory of rotating fluids. Cambridge University Press, Cambridge
4. Proudman J (1916) On the motion of solids in liquids possessing vorticity. Proc Roy Soc A 92:408–424
5. Taylor GI (1921) Experiments with rotating fluids. Proc Roy Soc A 100:114–121
6. Taylor GI (1923) Experiments on the motion of solid bodies in rotating fluids. Proc Roy Soc A 104:213–218
7. Montgomery RB (1937) A suggested method for representing gradient flow in isentropic surfaces. Bull Am Meteorol Soc 18:210–212
8. Ekman VW (1905) On the influence of the Earth's rotation on ocean-currents. Arkiv för Metamatik Astronomi och Fysik 2(11):1–52
9. Stewartson K (1957) On almost rigid rotations. J Fluid Mech 3:17–26
10. Stewartson K (1966) On almost rigid rotations. Part 2. J Fluid Mech 26:131–144
11. Hartmann J, Lazarus F (1937) Experimental investigations on the flow of mercury in a homogeneous magnetic field. K Dan Vidensk Selsk Mat-Fys Medd 15(7):1–45
12. Shercliff JA (1953) Steady motion of conducting fluids under transverse magnetic fields. Proc Camb Phil Soc 49:136–144
13. Kulikovskii AG (1968) Slow steady flows of a conducting fluid at high Hartmann numbers. Izv Akad Nauk SSSR Mekh Zhidk i Gaza 3:3–10
14. Holroyd RJ, Walker JS (1978) A theoretical study of the effect of wall conductivity, non-uniform magnetic fields and variable-area ducts on liquid-metal flows at high Hartmann numbers. J Fluid Mech 84(3):471–495
15. Alboussière T (2004) A geostrophic-like model for large-Hartmann-number flows. J Fluid Mech 521:125–154
16. Munk WH (1950) On the wind-driven ocean circulation. J Meteor 7(2):79–93
17. Stommel H (1948) The westward intensification of wind-driven ocean currents. Trans Am Geophys Union 29:202–206
18. Walker JS, Ludford GSS (1972) Three-dimensional MHD duct flows with strong transverse magnetic fields. Part 4. Fully insulated, variable-area rectangular ducts with small divergences. J Fluid Mech 56(3):481–496
19. Bühler L, Molokov S (1994) Magnetohydrodynamic flows in ducts with insulating coatings. Magnetohydrodynamics 30:439–447
20. Molokov S (2002) Evolution of a free surface in a strong vertical magnetic field. In: Proc 5th Int Conf on Fundamental and Applied MHD (PAMIR), Ramatuelle, France, 16-20 Sept 2002 2:65–70
21. Pothérat A, Sommèria J, Moreau R (2005) Numerical simulations of an effective two-dimensional model for flows with a transverse magnetic field. J Fluid Mech 534:115–143
22. Dellar PJ (2004) Quasi-two-dimensional liquid-metal magnetohydrodynamics and the anticipated vorticity method. J Fluid Mech 515:197–232
23. Lingwood RJ, Alboussière T (1999) On the stability of the Hartmann layer. Phys Fluids 11(8):2058–2068

24. Alboussière T, Lingwood RJ (2000) A model for the turbulent Hartmann layer. Phys Fluids 12(6):1535–1543
25. Rhines PB (1975) Waves and turbulence on a beta plane. J Fluid Mech 69:417–443